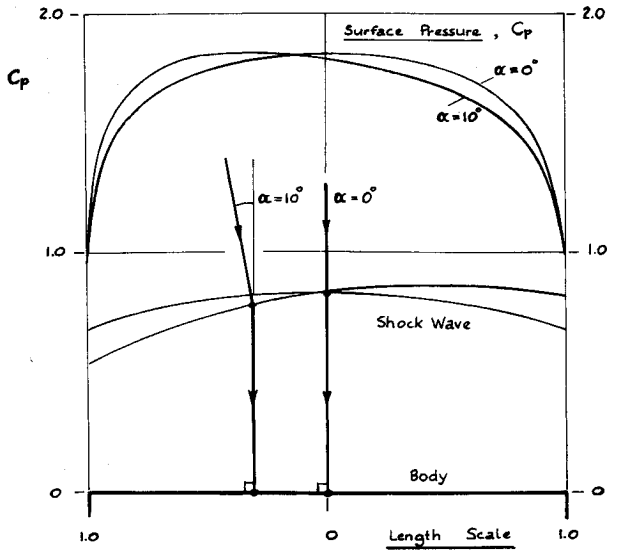

Fig. 2 Solution for supersonic flat plate; $M = 8.2$, $\gamma = 1.4$.

initial value of shock standoff distance. For plane bodies at incidence, the position of the stagnation point is also unknown, but can nominally be found by using the regularity conditions at both upper and lower sonic points. However, the problem is less complicated in a one strip analysis. Brong and Leigh,[11] have shown that for this case the stagnation streamline is a straight line normal to the body surface. Thus, for a given stagnation point the slope of the stagnation streamline and hence of the tangent to the shock wave can be found by simple plane shock theory. For a flat-faced blunt body (Fig. 1), therefore, both of these angles are known initially. Now, the regularity condition at the sonic point is in general controlled by an expression of the form

$$dv_{so}/ds = N/D$$

where D contains $c^{*2} - v_{so}^2$ and must be zero at a sonic point, and where N must be finite at a sharp corner, and zero at a smooth corner. Thus, this determines the basis upon which iteration is performed if it is necessary to search for the stagnation point shock standoff distance.

However, for a sharp cornered flat-faced plane body at arbitrary incidence, similarity requires that the body shape and size have no influence on the solution. Consequently, a solution can be obtained immediately for any assumed or unit shock standoff distance, by integrating from the stagnation point found by the method of Brong and Leigh until the sonic condition is satisfied. Although this can be termed an indirect rather than direct solution, since the body is found for a given initial shock, the direct solution for a given body size can in fact be found by simple scaling of lengths in the nominally indirect answer. Using about 250 integration steps on each side of the body, computing time on a CDC 6600 is about 10 sec. Some results are shown in Fig. 2.

References

[1] Belotserkovskii, O. M. and Chushkin, P. I., "The Numerical Solution of Problems in Gasdynamics," *Basic Developments in Fluid Dynamics*, Vol. 1, M. Holt, Ed., Academic Press, New York, 1965, pp. 55–73.

[2] Belotserkovskii, O. M., "Supersonic Flow Around Blunt Bodies," TT F-453, June 1967, NASA.

[3] Ware, R. C. and Archer, R. D., "An Evaluation of the First Order Approximation to the Direct Supersonic Blunt Body Problem," *Conference on Hydraulics and Fluid Mechanics*, The Institution of Engineers, Australia, Preprint, 1968, pp. 232–238.

[4] Xerikos, J. and Anderson, W. A., "Blunt Body Integral Method for Air in Thermodynamic Equilibrium," *AIAA Journal*, Vol. 3, No. 8, Aug. 1965, pp. 1531–1533.

[5] Holt, M., "Direct Calculation of Pressure Distribution on Blunt Hypersonic Nose Shapes with Sharp Corners," *Journal of the Aerospace Sciences*, Vol. 28, No. 11, Nov. 1961, pp. 872–877.

[6] Traugott, S. C., "An Approximate Solution of the Direct Supersonic Blunt Body Problem for Arbitrary Axisymmetric Shapes," *Journal of the Aerospace Sciences*, Vol. 27, No. 5, May 1960, pp. 361–370.

[7] Archer, R. D. and Hermann, R., "Supersonic and Hypersonic Flow of an Ideal Gas Around an Elliptic Nose," *AIAA Journal*, Vol. 3, No. 5, May 1965, pp. 987–988.

[8] Poon, N. H., "Inviscid Supersonic and Hypersonic Gas Flow Around Ellipsoids," M.Eng.Sc. thesis, 1970, University of New South Wales, Australia.

[9] McLean, G. R., "Inviscid Hypersonic Flow over Power Law Bodies by the Method of Integral Relations," B.E. thesis, 1967, University of New South Wales, Australia.

[10] Seach, B. C., "A Study of the Supersonic Blunt Body Problem," M.Eng.Sc. thesis, 1971, University of New South Wales, Australia.

[11] Brong, E. A. and Leigh, D. C., "Method of Belotserkovskii for Axisymmetric Blunt Body Flows," *AIAA Journal*, Vol. 2, No. 10, Oct. 1964, pp. 1852–1853.

Bending of an Orthotropic Cantilever

R. SIERAKOWSKI*
University of Florida, Gainesville, Fla.

AND

R. S. VAN HUYSEN† AND J. L. KRAHULA‡
Rensselaer Polytechnic Institute of Connecticut, Hartford, Conn.

THE shear stress distribution at composite beam interfaces is a problem of continuing concern to materials design engineers. In order to develop insight into the important parameters involved in evaluating such materials, improved analytical techniques are necessary for studying experimental results and providing useful design guidelines.

In a previous paper,[1] the plane stress solution applicable to a thin-walled cantilever beam with end load has been discussed. The present paper extends the preceding result to include the influence of beam width for the Saint Venant solution to the bending of a composite orthotropic beam, Fig. 1.

Using a semi-inverse technique we consider the Saint Venant solution for bending of a composite orthotropic cantilever beam Fig. 1 subject to the elastic field equations and the following stress and strain conditions[2]:

$$\begin{aligned} &\tau_{xy} = \sigma_x = \sigma_y = 0 \\ &\tau_{xz} = \tau_{xz}(x,y), \quad \tau_{yz} = \tau_{yz}(x,y), \quad \sigma_z = E_z \varepsilon_z \\ &\varepsilon_z = c_2 zx + c_3 x + c_5 z + c_6 \end{aligned} \tag{1}$$

The strain displacement equations, the equation of equilibrium and the substitution

$$\bar{w}(x,y) = Dx^3 + Fxy^2 + \alpha x^2 + \beta y^2 + w(x,y) \tag{2}$$

yield the desired equations

$$\begin{aligned} \bar{w} = {} & [-E_z/G_{zx} + \nu_{zx}](c_2/6)x^3 + \nu_{zy}(c_2/2)x^2 y + \\ & [-E_z/G_{xz} + \nu_{zx}](c_5/2)x^2 + \nu_{zy} c_5 y^2/2 + w(x,y) \end{aligned} \tag{3a}$$

Received November 22, 1971; revision received January 18, 1972. The authors wish to acknowledge the assistance of C. Myers who wrote the computer code for the numerical analysis.

Index categories: Structural Static Analysis; Structural Composite Materials.

* Associate Professor, Engineering Science and Mechanics.

† Graduate Student.

‡ Professor of Engineering Mechanics. Associate Fellow AIAA.

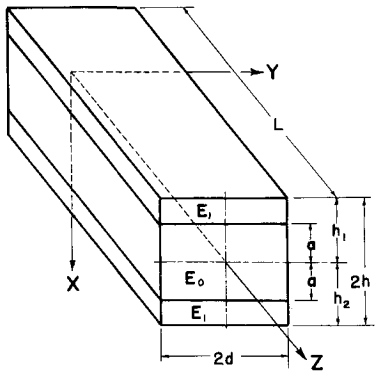

Fig. 1 Composite geometry configuration.

$$G_{zx}\partial^2 w/\partial x^2 + G_{zy}\partial^2 w/\partial y^2 = 0 \tag{3b}$$

$$\gamma_{zy} = \partial w/\partial y, \quad \tau_{zy} = G_{zy}\gamma_{zy} \tag{3c}$$

$$\gamma_{zx} = \partial w/\partial x + [v_{zy}y^2 - E_z x^2/2G_{zx}]c_2 - E_z c_5 x/G_{zx},$$

$$\tau_{zx} = G_{zx}\gamma_{zx} \tag{3d}$$

as well as equations for the displacements u and v. The preceding equations contain only the unknown function $w(x, y)$.

For the composite beam shown in Fig. 1, $w(x,y)$ may be found by assuming[3]

$$w_i = \sum_{m=0}^{\infty} X_i(x)\cos\alpha_m y + A_i x + B_i \tag{4}$$

where $\alpha_m = m\pi/d$ and the subscript i refers to the regions as shown in Fig. 1. The unknown constants and function are obtained using the equations of equilibrium (3b) and the boundary conditions at the outer surface of the beam as well as continuity at the interior interface of the beam. These conditions are expressed by,

$$\tau_{zy} = 0 \quad \text{at} \quad y = \pm d \tag{5a}$$

$$\tau_{zx} = 0 \quad \text{at} \quad x = h_1 \quad \text{and} \quad x = -h_2 \tag{5b}$$

$$\bar{w}_1 = \bar{w}_0, \quad \tau_{zx_1} = \tau_{zx_0} \quad \text{at} \quad x = a \tag{5c}$$

$$\bar{w}_2 = \bar{w}_0, \quad \tau_{zx_2} = \tau_{zx_0} \quad \text{at} \quad x = -a \tag{5d}$$

The equilibrium conditions at any section z yield the constants $c_2 - c_6$ in terms of the external load V.

The problem of a three-layered symmetric isotropic beam, with upper and lower layers having different properties from that of the middle layer, has been solved in detail. For purposes of brevity, the calculated stress resultants and associated calculations have been omitted, but are available upon request from the authors.

Results and Discussion

As a numerical example, the following three types of beams are considered: a) thin, $d/h = 0.2$, b) rectangular, $d/h = 1.0$, and c) platelike, $d/h = 5.0$. Values for the stresses have been computed for core dimensions of $a/h = \frac{1}{4}, \frac{1}{2}, \frac{3}{4}$ and for $G_0 = 0.185\times10^6$ psi, $G_1 = 3.75\times10^6$ psi, $E_0 = 0.5\times10^6$ psi, $E_1 = 10\times10^6$ psi, $v_0 = 0.35$, $v_1 = 0.33$. The numerical values were selected in order to compare the thin beam solution generated in the present development with that presented in Ref. 1.

Graphical results for the shear stress distribution for a beam configuration of type b are shown in Figs. 2 and 3. It is noted that a comparison of the present transverse shear results (τ_{xz}) with those obtained in Ref. 1, based upon a plane stress formulation, are similar to within five place digital accuracy. The graphical plots of τ_{xz} for beam types a, b are coincident. The variation of the other in plane shear force (τ_{yz}) is shown three dimensionally for beam type b in Figs. 3a, 3b, and 3c for increasing x/a and y/d. For the case considered, the absolute magnitude of the largest value of τ_{yz} is an order of magnitude smaller than τ_{xz}. This maximum value of τ_{yz} occurs in the facing material (E_1), for $d/a = 1$, $a/h = \frac{4}{3}$. In general, it is found

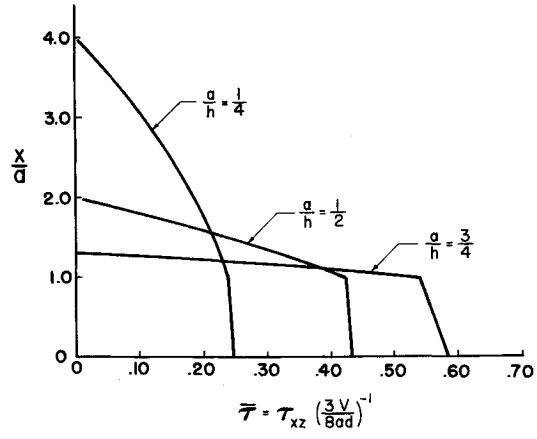

Fig. 2 Graph of vertical dimensionless stress $\bar{\tau}_{xz}$ vs x/a.

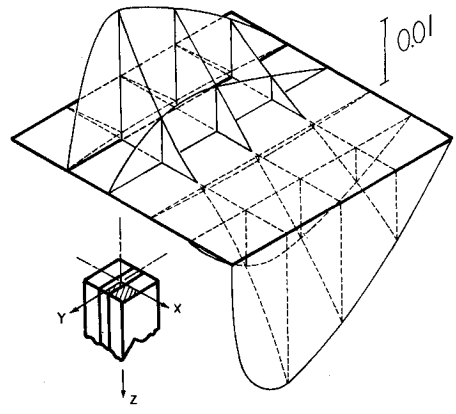

Fig. 3a Graph of horizontal dimensionless stress $\bar{\tau}_{yz}$ vs the cross section of dimensions for $a/h = \frac{1}{4}$.

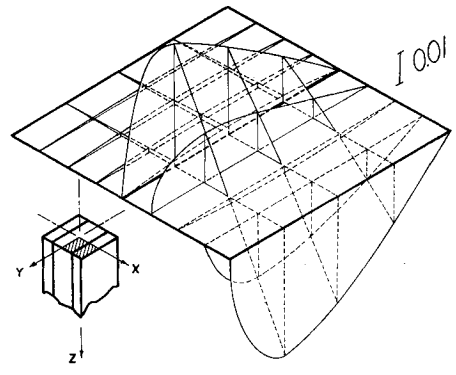

Fig. 3b Graph of horizontal dimensionless stress $\bar{\tau}_{yz}$ vs the cross section dimensions for $a/h = \frac{1}{2}$.

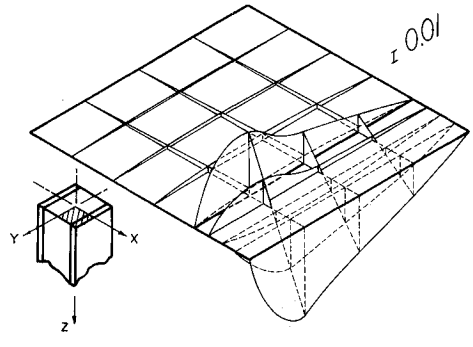

Fig. 3c Graph of horizontal dimensionless stress $\bar{\tau}_{yz}$ vs the cross section dimensions for $a/h = \frac{3}{4}$.

that the magnitude of τ_{yz} increases as the beam configuration changes to a plate geometry and as the core thickness increases.

Several points have been considered in the numerical calculations. These relate to rate of convergence of the numerical results and breakdown in usefulness of the developed equations as the geometrical configuration is changed from a beam to a platelike structure. The former problem has been examined by comparing sums of various numbers of terms in the series solution with the required accuracy of the numerical solution at the beam boundary surfaces. It has been found that for geometrical configurations of the type *a, b,* one and three term summations, respectively, for the core dimensions considered, are sufficient to generate three place numerical accuracy. As noted earlier, the solution for τ_{xz} as generated for the thin beam case ($d/h = 0.2$) coincides with that presented in Ref. 1, based upon a two-dimensional elastic solution. In the case of platelike geometries, separate discussion is required in that the rate of numerical convergence for the physical quantities of interest changes with both d/h and a/h. As both of these parameters are increased, the required number of terms, to obtain comparable numerical accuracy as described above, requires an increasing number of terms. For example, for the case of $d/h = 10$ and core dimensions of $a/h < \frac{1}{2}$, upwards of sixty terms are required. Larger numbers of terms are required for a/h ratios $\geq \frac{1}{2}$. It is possible, however, to develop numerical techniques, which could provide useful guides for determining the numerical accuracy of the stresses by preselecting a maximum number of cutoff terms to achieve a desired numerical accuracy. The width and core dimensions could be appropriately varied with the number of cutoff terms selected as a parameter. Composite beams with more than three lamina may be solved in the manner indicated previously.

References

[1] Sierakowski, R. L. and Ebcioglu, I. K., "On Interlaminar Shear Stresses in Composites," *Journal of Composite Materials,* Vol. 4, No. 1, Jan. 1970, pp. 144–149.

[2] Lauterbach, G., Peppin, R. J., Schapiro, S., and Krahula, J. L., "Finite Element Solution for Saint Venant Bending," *AIAA Journal,* Vol. 9, No. 3, March, 1971, pp. 525–527.

[3] Love, A. E. H., *A Treatise on the Mathematical Theory of Elasticity,* 4th ed., Dover, New York, 1944, pp. 329–364.

Inhibition of the Ablation Rate of Graphite by Gaseous Chlorine

HOWARD G. MAAHS*
NASA Langley Research Center, Hampton, Va.

Introduction

RESULTS from a number of laboratory experiments reported in the literature indicate that chlorine gas[1-3] or various chlorinated compounds[3-6] effectively inhibit the oxidation of carbon or graphite in either pure oxygen[1,3] or in air.[2,4-6] The temperature range over which an inhibiting effect has been reported is from 733°K to 2033°K (Ref. 1). The mechanism generally assumed for this inhibition is that chlorine (or the chlorinated compound) is strongly chemisorbed on the surface blocking oxygen from reaching many of the active sites.[1-3,5,6] Experimental evidence offered in support of this mechanism is that the carbon or graphite surface, after oxidation in the presence of chlorine or chlorinated compounds as inhibitors, has a different character than it does after oxidation in the absence of inhibitors.[1,5,6] Also, it has been reported in other studies[7,8] that chlorine is irreversibly chemisorbed on carbon and graphite at least over the temperature range 77°K to 770°K, with appreciable chlorine remaining on the carbon surface even after heating to 1470°K in vacuum.[7]

If chlorine, in addition to inhibiting the rate of oxidation of graphite, could also be shown to be effective in inhibiting the over-all rate of ablation of graphite in a high-temperature, supersonic environment, this could have significant implications for the design of thermal protection systems in which the rapid ablation rate of carbon or graphite is a serious consideration. Accordingly, the present study was undertaken to investigate the possible inhibiting effect of chlorine on graphite ablation. Of primary interest were the concentration levels of chlorine necessary for inhibition, and the magnitudes of inhibition which might reasonably be attained.

Ablation Performance Measurements

Many of the experimental details of the ablation performance measurements are similar to those described in Ref. 9, and therefore will be described only briefly here. The ablation environment consisted of a nominal Mach 2 test stream with a nominal enthalpy of 2.29 Mjoule/kg and a stagnation pressure of 5.7 atm, obtained in an arc-heated air stream. Heating rates were nominally 547 w/cm^2 at the stagnation point; however, due to difficulties encountered in making the heating rate measurements, and also possibly in maintaining constant conditions in the arc heater itself, actual measured heating rates ranged from 517 w/cm^2 to 579 w/cm^2, and corresponding enthalpies ranged from 2.18 Mjoule/kg to 2.20 Mjoule/kg.

Test specimens were ATJ graphite machined into 1.270-cm-diam hemisphere cylinders, 1.905 cm long, with nose radii of 0.635 cm. The direction of preferred crystallite orientation was normal to the axis of the specimens. The specimens were insulated from their holders during test. Steady-state stagnation-point surface temperatures were measured with a continuous-recording photographic pyrometer, and linear stagnation-point mass loss rates were determined from motion picture film records of the eroding specimens with the aid of a motion analyzer. Representative surface temperature was taken as the steady-state maximum temperature attained during the run; mass loss rate was determined from a least-squares slope of the linear portion of the specimen length decrease with time by multiplying it by the bulk density. Ablation performance measurements were made in pure, dry air, and in mixtures of chlorine in dry air in the concentrations 0.01%, 0.043%, 0.107%, 0.41%, and 1.05% (volume percent). Replicate runs were made at each gas composition.

Effects of Chlorine Addition

The results of the ablation performance measurements are shown in Fig. 1 in terms of mass loss rate and surface temperature as functions of the test stream composition. To facilitate comparison, the mass loss rate and surface temperature data obtained in a test stream of pure air (chlorine concentration of 0%) are indicated by the horizontal bounds drawn across the entire figure. Figure 1a illustrates the inhibiting effect of small amounts of chlorine on mass loss rate, indicating that as chlorine concentration increases mass loss rate decreases. At a chlorine concentration of only 1%, mass loss rate is reduced by almost one-third of that in pure air. Figure 1b reveals that small amounts of chlorine depress the surface temperature below that when no chlorine is present. Such surface temperature depression due to chlorine addition has been previously reported,[1] and is consistent with the fact that the oxidation of carbon is exothermic: a slower rate of reaction tends to reduce surface temperature because heat is being generated at a slower rate.

A particularly intriguing aspect of the temperature data in Fig. 1b is that they pass through a maximum with increasing chlorine concentration. Since these temperature data are believed to be accurate to within approximately 50°K, this maximum cannot be easily ascribed to experimental error. Yet, no alternative

Received December 1, 1971.
Index category: Material Ablation.
* Aerospace Technologist.